Zinc-Dependent Structural Stability of Human Sonic Hedgehog

Eric S. Day[‡,§] and Dingyi Wen,[‡,§] Ellen A. Garber,[‡] Jin Hong,[||] Lena S. Avedissian,[‡] Paul Rayhorn,[‡] Weihong Shen,[‡] Chenhui Zeng,[‡] Voilaine R. Bailey,[‡] Jennifer O. Reilly,[⊥] Julie A. Roden,[‡] Claire B. Moore,[‡] Kevin P. Williams,[‡] Alphonse Galdes,[‡] Adrian Whitty,[‡] and Darren P. Baker*[,‡]

Biogen Inc., 14 Cambridge Center, Cambridge, Massachusetts 02142, 77 Pine Ridge Drive, Ayer, Massachusetts 01432, and Ontogeny Inc., 45 Moulton Street, Cambridge, Massachusetts 02139

Received May 3, 1999; Revised Manuscript Received August 18, 1999

ABSTRACT: The role of the zinc site in the N-terminal fragment of human Sonic hedgehog (ShhN) was explored by comparing the biophysical and functional properties of wild-type ShhN with those of mutants in which the zinc-coordinating residues H140, D147, and H182, or E176 which interacts with the metal ion via a bridging water molecule, were mutated to alanine. The wild-type and E176A mutant proteins retained 1 mol of zinc/mol of protein after extensive dialysis, whereas the H140A and D147A mutants retained only 0.03 and 0.05 mol of zinc/mol of protein, respectively. Assay of the wild-type and mutant proteins in two activity assays indicated that the wild-type and E176A mutant proteins had similar activity, whereas the H140A and D147A mutants were significantly less active. These assays also indicated that the H140A and D147A mutants were susceptible to proteolysis. CD, fluorescence, and ^{1}H NMR spectra of the H140A, D147A, and E176A mutants measured at 20 or 25 °C were very similar to those observed for wild-type ShhN. However, CD measurements at 37 °C showed evidence of some structural differences in the H140A and D147A mutants. Guanidine hydrochloride (GuHCl) denaturation studies revealed that the loss of zinc from the H140A and D147A mutants destabilized the folded proteins by ∼3.5 kcal/mol, comparable to the effect of removing zinc from wild-type ShhN by treatment with EDTA. Thermal melting curves of wild-type ShhN gave a single unfolding transition with a midpoint T_m of ∼59 °C, whereas both the H140A and D147A mutants displayed two distinct transitions with T_m values of 37−38 and 52−54 °C, similar to that observed for EDTA-treated wild-type ShhN. Addition of zinc to the H140A and D147A mutants resulted in a partial restoration of stability against thermal and GuHCl denaturation. The ability of these mutants to bind zinc was confirmed using a fluorescence-based binding assay that indicated that they bound zinc with K_d values of ∼1.6 and ∼15 nM, respectively, as compared to a value of ≤100 pM for wild-type ShhN. The properties of the E176A mutant were indistinguishable from those of wild-type ShhN in all biophysical and functional assays, indicating that this residue does not contribute significantly to stabilization of the zinc-binding site and that ShhN does not require hydrolase activity for in vitro biological function.

Hedgehog proteins constitute a family of extracellular signaling molecules that are involved in the regulation of invertebrate and vertebrate embryo development (*2*). Vertebrate organisms express multiple forms of hedgehog, and in mammals three homologues, Sonic hedgehog (Shh),[1] Indian hedgehog (Ihh), and Desert hedgehog (Dhh), have been identified (*1*, *3*). Shh plays an important role in numerous developmental processes, including the differentiation of floor plate and motor neurons in the neural tube (*4*, *5*), the induction of midbrain dopaminergic neurons (*6*, *7*) and basal forebrain cholinergic neurons (*8*), the branching of the developing lungs (*9*), as well as the development of the retina (*10*, *11*). The importance of Shh for development is underscored by the severity of malformation associated with mutations in the *Shh* gene. The resulting human disorder, holoprosencephaly, is phenotypically heterogeneous with symptoms ranging from mild facial dysmorphia and microcephaly to the complete failure of the left and right hemispheres of the brain to separate, cyclopia, the formation of a primitive nasal proboscis, and midfacial clefting in the most severe cases (*12*−*14*). Similarly, knockout of the *Shh* gene in mice leads to disruption in the formation of the notochord and floorplate, cyclopia, the absence of the spinal column and most of the ribs, and in the reduction of brain and limb size (*15*).

Shh is synthesized as a 45-kDa precursor protein that is cleaved autocatalytically to yield a 20-kDa N-terminal fragment (ShhN, residues 24−197 in the human gene sequence) with a cholesterol molecule covalently attached to the C-terminal glycine, and a 25-kDa C-terminal fragment

* Corresponding author. Tel.: 617-679 2165. Fax: 617-679 2304. E-mail: darren_baker@biogen.com.
‡ Biogen Inc.
§ Contributed equally to this work.
|| Ayer, MA.
⊥ Ontogeny Inc.

[1] Abbreviations: Dhh, Desert hedgehog; ESI−MS, electrospray ionization−mass spectrometry; GuHCl, guanidine hydrochloride; hh, hedgehog; Ihh, Indian hedgehog; NMR, nuclear magnetic resonance; PBS, phosphate-buffered saline; PBST, PBS containing 0.1% Triton X-100; ppm, parts per million; SDS−PAGE, sodium dodecyl sulfate−polyacrylamide gel electrophoresis; Shh, Sonic hedgehog; ShhN, N-terminal fragment of Sonic hedgehog.

10.1021/bi9910068 CCC: $18.00
Published on Web 10/23/1999

that is responsible for peptide bond cleavage and for catalyzing the addition of the cholesterol (*16*−*20*). Recent studies have also shown that human ShhN is modified with a palmitoyl moiety that is covalently attached to the α-amine group of the N-terminal cysteine (C24[2]) (*20*). ShhN is responsible for all known Shh-dependent signaling activities.

The crystal structure of murine ShhN has been determined (*21*). Murine ShhN contains a single zinc ion that is bound at the bottom of a solvent-accessible cleft. The zinc is coordinated by the side chains of H141, D148, and H183 with a water molecule acting as the fourth ligand (*21*). The tertiary structure of murine ShhN is very similar to that of the catalytic domain of *N*-acyl-D-Ala-D-Ala carboxypeptidase from *Streptomyces albus* with the identity and geometry of the zinc-coordinating residues being invariant (*22*−*24*). Similarly, two histidines and an aspartate residue coordinate the zinc in D-Ala-D-Ala dipeptidase from *Enterococcus faecium* (*25*, *26*). The coordination of zinc in murine ShhN is also similar to that found in *Bacillus thermoproteolyticus* thermolysin (*27*, *28*) and in bovine carboxypeptidase A (*29*−*31*), proteases in which the zinc is coordinated by two histidines and a glutamate residue. In thermolysin, carboxypeptidase A, and D-Ala-D-Ala dipeptidase, an essential aspartate or glutamate residue lies close to the zinc and, during catalysis, is believed to act as a general base by activating the zinc-bound water molecule for attack on the protein-bound substrate (*25*, *30*). Likewise, E177 in murine ShhN is located close to the zinc and is hydrogen-bonded to the zinc-bound water molecule (*21*). Since murine ShhN is structurally homologous to a number of zinc-dependent hydrolases, it has been proposed that the protein may have intrinsic hydrolase activity, although to date no such activity has been identified (*21*). It is unclear whether the presence of zinc in murine ShhN is indicative of hydrolase activity, whether the function of the zinc is to stabilize the protein fold, or both.

To address this question and to determine the importance of the zinc-coordinating residues and the proposed catalytic glutamate in human ShhN, we have used site-specific mutagenesis to replace H140, D147, E176, and H182 with alanine. These residues are homologous to H141, D148, E177, and H183, respectively, in murine ShhN and differ in sequence number only because the murine protein contains an additional amino acid in its signal sequence (*1*). Although the crystal structure of human ShhN has not been reported, it is likely to be essentially identical to that of the murine protein since they differ in sequence by only one residue; S67 in human ShhN is replaced in murine ShhN by threonine.[3] In addition to being conserved in murine and human ShhN, residues corresponding to H141, D148, E177, and H183 in murine ShhN are absolutely conserved in murine and human Dhh, human Ihh, rat Shh, and mosquito hh but not in *Drosophila melanogaster* hh (*21* and references therein).

Here we report the biophysical and biological characterization of the wild-type and H140A, D147A, E176A, and H182A mutants of human ShhN and discuss the effects of the mutations on the structure, stability, and biological activity of the proteins.

EXPERIMENTAL PROCEDURES

Materials. DNase (grade II) and dispase were purchased from Boehringer Mannheim; sodium mono- and dihydrogenphosphate, EDTA, HPLC-grade water, HCl, and HNO_3 (Optima grade) and the $ZnCl_2$ reference solution for atomic absorption spectroscopy were purchased from Fisher Scientific; *o*-phenanthroline, metal-free water, and $ZnSO_4$ were purchased from Fluka; Cy-3-conjugated streptavidin was purchased from Jackson Immunoresearch; DMEM/F-12 serum-free medium was purchased from Life Technologies Inc.; trifluoroacetic acid and 8 M guanidine hydrochloride (GuHCl) were purchased from Pierce Chemical Co.; HPLC-grade acetonitrile, and HPLC-grade water for zinc analysis were purchased from J. T. Baker; SP-Sepharose and Phenyl Sepharose (high sub) Fast Flow resins were purchased from Pharmacia; NTA-Ni^{2+} agarose was purchased from Qiagen; imidazole, phenylmethylsulfonyl fluoride, isopropylthiogalactoside, ampicillin, and hyaluronidase were purchased from Sigma; calf-intestine enterokinase was purchased from Biozyme Laboratories International Ltd.; anhydrous 99.999% $ZnCl_2$ for formulating purified proteins was purchased from Alpha; Magnesium Green was purchased from Molecular Probes; and biotinylated horse anti-mouse IgG was purchased from Vector Laboratories. The murine anti-chicken islet-1 monoclonal antibody 39.4D5, developed by Dr. Thomas Jessell, was obtained from the Developmental Studies Hybridoma Bank developed under the auspices of the NICHD and maintained by the University of Iowa, Department of Biological Sciences, Iowa City, IA. The plasmid p6H-SHH, containing the cDNA for wild-type human *ShhN*, was kindly provided by Dr. David Bumcrot (Ontogeny Inc.).

Construction of the H140A, D147A, E176A, and H182A Mutants by Site-Specific Mutagenesis. The mutational changes in human ShhN were introduced by unique site elimination mutagenesis of plasmid pEAG543, a pUC-derived vector containing the cDNA for wild-type *ShhN* flanked by *Not*I sites, using a Pharmacia kit following the manufacturer's recommended protocol. Mutations were confirmed by dideoxy sequencing. After each mutation had been verified, a small fragment of the gene carrying the mutation was recloned into the plasmid p6H-SHH, a derivative of plasmid pET11d that carries the wild-type human *ShhN* cDNA starting at C24 and extending to G197, followed by tandem termination codons, and cloned as an *Nco*I−*Xho*I fragment so that the *ShhN* cDNA is downstream of sequences encoding six consecutive histidine residues and a DDDDK enterokinase cleavage site. For the H140A, D147A, E176A, and H182A mutations, a 526 base pair (bp) *Rsr*II−*Not*I fragment was isolated and subcloned with kinase-treated, annealed *Not*I−*Xho*I linkers into a 5702 bp *Xho*I−*Rsr*II fragment of p6H-SHH. Verification of the plasmid construction was accomplished by restriction analysis, and each mutation was verified for a

[2] The one letter amino acid abbreviation system is used throughout. The numbering system used is consistent with that published elsewhere in which the N-terminal amino acid of the peptide leader sequence is residue number 1 and where C24 becomes the N-terminal residue of the mature protein after removal of the leader sequence.

[3] Although the original paper reporting the sequence comparison of the murine and human *Shh* genes (*1*) indicates that S67 and K121 in human ShhN are replaced in murine ShhN by threonine and arginine, respectively, the latter substitution has subsequently been found to be in error (Dr. Andrew McMahon, personal communication). Both proteins therefore have a lysine at the position corresponding to K121 of human ShhN.

second time by dideoxy sequencing through a 585 bp *Nco*I−*Not*I restriction fragment encompassing the entire subcloned fragment. No mutations, other than the desired ones, were found within the sequences of the subcloned fragments. In this fashion, plasmids pEAG631, pEAG632, pCM304, and pEAG633 were constructed, carrying the H140A, D147A, E176A, and H182A mutations, respectively.

Wild-Type and Mutant Protein Overproduction. The wild-type and mutant proteins were isolated from *Escherichia coli* strain BL21/DE3/plysS (Stratagene, La Jolla, CA) containing the appropriate plasmid. To aid in the purification of the proteins, the constructs were engineered to contain a hexahistidine tag and an enterokinase cleavage site (DDDDK) immediately upstream of the N-terminal cysteine residue (C24). Cells containing mutant *ShhN* cDNA were grown at 37 °C in TB-MGB medium containing 100 μg/mL ampicillin in a 10 L fermentor controlled for aeration and pH. The fermentor was inoculated with 200 mL of a culture grown overnight in TB-MGB medium containing 100 μg/mL ampicillin, and then isopropylthiogalactoside (IPTG) was added to 0.5 mM when the culture reached an optical density at 550 nm of 0.6−0.8. The cells were harvested by centrifugation 2−3 h after the addition of IPTG, and the cell pellets were stored at −70 °C. Cells containing wild-type *ShhN* cDNA were grown in a 500 L fermentor at the Waksman Institute, Rutgers University, essentially as described above. Expression of ShhN was confirmed by reducing SDS−PAGE by comparing cell lysates prepared immediately before the addition of IPTG with those prepared at the time of harvest.

Wild-Type and Mutant Protein Purification. Cells were lysed and the proteins purified to homogeneity at 0−4 °C, except for purification on Phenyl Sepharose, which was carried out at room temperature. Cell pellets were thawed and resuspended in 4 mL of 25 mM Na_2HPO_4, pH 8.0, 150 mM NaCl, 1 mM EDTA, 0.5 mM DTT, and 1 mM phenylmethylsulfonyl fluoride per gram of cells and then disrupted by two passages through a Rannie (Copenhagen, Denmark) high-pressure homogenizer operated at 700 psi. Cell debris was then removed by centrifugation for 30 min at 19000*g*. The cell-free extract was adjusted to pH 6.0, and the sample was loaded onto a column of SP-Sepharose Fast Flow resin equilibrated with 25 mM Na_2HPO_4, pH 5.5, 150 mM NaCl, and 0.5 mM DTT. Once loaded, the column was washed with the equilibration buffer, followed by 25 mM Na_2HPO_4 pH 5.5, 300 mM NaCl, and 0.5 mM DTT, before a final wash with 25 mM Na_2HPO_4, pH 5.5, 400 mM NaCl, and 0.5 mM DTT. ShhN was eluted with 25 mM Na_2HPO_4, pH 5.5, 800 mM NaCl, and 0.5 mM DTT. Fractions containing ShhN were pooled and filtered through a 0.2-μm filter. The SP-Sepharose pool was mixed with sufficient 5 M NaCl, 1 M imidazole, pH 7.0, 1 M Na_2HPO_4, pH 8.0, and 1 M DTT to bring the concentrations to 1 M, 20 mM, 25 mM, and 0.5 mM, respectively. The sample was loaded onto a column of NTA-Ni^{2+} agarose equilibrated with 25 mM Na_2HPO_4, pH 8.0, 1 M NaCl, 20 mM imidazole, and 0.5 mM DTT. Once loaded, the column was washed with the equilibration buffer before bound protein was eluted with 25 mM Na_2HPO_4, pH 8.0, 1 M NaCl, 200 mM imidazole, and 0.5 mM DTT into tubes containing sufficient 1 M DTT to bring the fractions to 0.5 mM with respect to the added reductant. Fractions containing ShhN were pooled. The NTA-Ni^{2+} agarose pool was equilibrated to room temperature, and an equal volume of either 2.5 M Na_2SO_4/0.5 mM DTT (wild-type protein) or 2 M Na_2SO_4/0.5 mM DTT (mutant protein) was added while swirling gently. The sample was loaded onto a column of Phenyl Sepharose 6 Fast Flow resin equilibrated with either 25 mM Na_2HPO_4, pH 8.0, 400 mM NaCl, 1.25 M Na_2SO_4, and 0.5 mM DTT (wild-type protein) or 25 mM Na_2HPO_4, pH 8.0, 400 mM NaCl, 1 M Na_2SO_4, and 0.5 mM DTT (mutant protein). Once loaded, the column was washed with the appropriate equilibration buffer before bound protein was eluted with 25 mM Na_2HPO_4, pH 8.0, 400 mM NaCl, and 0.5 mM DTT. Fractions containing ShhN were pooled. The hexahistidine tag was then removed from the proteins using calf-intestine enterokinase. The Phenyl Sepharose pool was diluted to 6 mg/mL with 25 mM Na_2HPO_4, pH 8.0, 400 mM NaCl, and 0.5 mM DTT, and 14 400 units (112 μg) of enterokinase was added per 10 mL of the ShhN solution. The sample was incubated at 28 °C for 2 h (wild-type, E176A, and H182A proteins) or 6 h (H140A and D147A proteins); times that were determined from pilot experiments to be the minimum required for >90% cleavage of the hexahistidine tag. The cleaved ShhN protein was separated from the uncleaved protein and the liberated tag on a column of NTA-Ni^{2+} agarose. The enterokinase-digested sample was mixed with sufficient 5 M NaCl and 1 M imidazole, pH 7.0, to bring the concentrations to 1 M and 20 mM, respectively. The sample was loaded onto a column of NTA-Ni^{2+} agarose equilibrated with 25 mM Na_2HPO_4, pH 8.0, 1 M NaCl, 20 mM imidazole, and 0.5 mM DTT. The flow through, containing the cleaved ShhN protein, and 5 column volume washes of the equilibration buffer were collected into a tube containing sufficient 1 M DTT to bring the solution to 0.5 mM with respect to the added reductant. The flow through and wash pool was mixed with 0.1 vol of 0.5 M MES, pH 5.0, and 9 vol of 5 mM Na_2HPO_4, pH 5.5, 150 mM NaCl, and 0.5 mM DTT. The sample was loaded onto a column of SP-Sepharose Fast Flow resin equilibrated with 5 mM Na_2HPO_4, pH 5.5, 150 mM NaCl, and 0.5 mM DTT. Once loaded, the column was washed with the equilibration buffer, followed by 5 mM Na_2HPO_4, pH 5.5, 300 mM NaCl, and 0.5 mM DTT. ShhN was eluted with 5 mM Na_2HPO_4, pH 5.5, 800 mM NaCl, and 0.5 mM DTT. Fractions containing ShhN were pooled. $ZnCl_2$ was added at a 10:1 molar ratio, and the protein was incubated for 2 h on ice. The zinc-treated protein was then dialyzed extensively against 5 mM Na_2HPO_4, pH 5.5, 150 mM NaCl, and 0.5 mM DTT. The dialyzed protein was filtered through a 0.2-μm filter, flash-frozen with liquid N_2, and stored at −70 °C.

Determination of Protein Concentration. The concentrations of the purified wild-type and mutant proteins were determined from absorbance measurements at 280 nm in 6 M GuHCl, using a calculated extinction coefficient of 26 030 L mol^{-1} cm^{-1} (32).

HPLC and Mass Spectrometry. Samples (20 μg) of the wild-type and mutant proteins were loaded at 1.4 mL/min onto a C_4 reverse-phase HPLC column (214TP104, 4.6 mm i.d. × 250 mm; Vydac, Hesperia, CA) equilibrated with 0.1% trifluoroacetic acid/5% acetonitrile. The column was developed with a linear 5−85% acetonitrile gradient in 0.1% trifluoroacetic acid over 30 min. Fractions containing protein were concentrated under vacuum and subjected to electrospray ionization−mass spectrometry (ESI−MS) using a

Micromass (Beverly, MA) Quattro II triple quadrupole mass spectrometer equipped with an electrospray ion source. Typically, a volume of 5 μL containing 5 pmol of HPLC-purified protein was infused directly into the ion source at a rate of 10 μL/min using 50% acetonitrile/0.1% formic acid as the solvent in the syringe pump. Scans were acquired throughout the sample infusion, and all mass spectral data were stored in profile mode and processed using the Micromass MassLynx data system.

Zinc Content Determination. Samples (1 mg) of the wild-type and mutant proteins were digested in 1 N HCl/1 N HNO_3 for 3 h at 100 °C in Teflon tubes. The samples were cooled and diluted with HPLC-grade water in acid-treated volumetric flasks, and the zinc content was determined immediately by atomic absorption spectroscopy using a Perkin-Elmer (Norwalk, CT) model 2380 atomic absorption spectrometer operated at 213.9 nm, 0.7 nm slit width, using a zinc lamp and an air−acetylene flame. A standard curve of $ZnCl_2$ was prepared at the same concentrations of HCl and HNO_3 as present in the protein samples. The zinc concentration of the last dialysis buffer was determined in an identical manner, and the residual zinc content of the buffer was deducted from the samples that contained protein.

Induction of Alkaline Phosphatase Expression in C3H10T1/2 Cells. The wild-type and mutant proteins were tested for activity in a cell-based assay measuring the induction of alkaline phosphatase expression in C3H10T1/2 cells (*33*). The assay was performed in a 96-well format, and samples were assayed in duplicate. Wild-type and mutant proteins, formulated in 5 mM Na_2HPO_4, pH 5.5, 150 mM NaCl, and 0.5 mM DTT, were first diluted with Dulbecco's modified Eagle's medium containing 10% fetal bovine serum, 2 mM glutamine, 100 unit/mL penicillin, 100 μg/mL streptomycin, 0.5 μg/mL $ZnSO_4$, and 142 μM 2-mercaptoethanol and then serially diluted down the plates into wells containing a culture medium/buffer mixture sufficient to maintain the same concentration of added Na_2HPO_4, NaCl, and DTT in all wells. After a 5-day incubation at 37 °C, the cells were lysed, and the level of alkaline phosphatase activity was measured at 405 nm using the chromogenic substrate *p*-nitrophenyl phosphate.

Induction of Islet-1 Expression in Chick Embryo Neural Plate Explants. Chick embryo neural plate explants were dissected from 8−10 somite stage chick embryos and cultured essentially as described (*34*, *35*) with the following modifications. The caudal most part of the embryo was removed and dissociated in a cocktail containing dispase, DNase, and hyaluronidase at 5 mg/mL, 20 μg/mL, and 10 μg/mL, respectively, for 10 min at 22 °C to remove mesenchymal tissue. The remaining tissue was removed and washed with 1% heat-inactivated fetal calf serum and placed in DMEM/F-12 serum-free medium. The intermediate zone of the neural plate was then removed and cultured in a three-dimensional collagen gel. ShhN proteins (1 μg/mL) or buffer control were added at the time of culture, and the explants (6−7 per sample) were incubated for 2 days at 37 °C. Explants were then fixed for 3 h in 1% paraformaldehyde; washed for 8 h at room temperature with PBS, pH 7.4; and then incubated overnight at 4 °C with the murine anti-chicken islet-1 monoclonal antibody 39.4D5 (1:100) in PBS, pH 7.4, and 0.1% Triton X-100 (PBST). The explants were then washed with PBST and incubated overnight at 4 °C with biotinylated horse anti-mouse IgG (1:200) in PBST. The explants were washed with PBST and then incubated with Cy-3-conjugated streptavidin (1:200) in PBST. The explants were finally washed with PBST and mounted on slides. Cells were observed by fluorescence microscopy, and the number of cells containing islet-1-positive nuclei were counted.

Circular Dichroism (CD) Spectroscopy. ShhN protein (7.2 μM) in 0.5 mM Na_2HPO_4, pH 5.5, 15 mM NaCl, and 50 μM DTT was analyzed with a JASCO (Tokyo, Japan) model J-715 spectropolarimeter with a 1 mm path length cuvette at either 20, 37, or 70 °C at a scan rate of 10 nm/min. Thermal denaturation was monitored at 215 nm with a linear temperature gradient of 0.5 °C/min, whereas GuHCl-induced denaturation was monitored at 222 nm at 20 °C (in each case the monitoring wavelength yielded the largest dynamic range between the native and denatured states). The concentration of GuHCl at which 50% of the protein is denatured ($[GuHCl]_{1/2D}$) was determined by plotting the free energy of unfolding (ΔG_D) versus the concentration of GuHCl ($\Delta G_D = a[GuHCl] + b$; $[GuHCl]_{1/2D} = -b/a$, where a is the slope and b is the y-intercept). ΔG_D was calculated using the following equation (*36*):

$$\frac{-\Delta G_D}{RT} = \ln \frac{[\theta] - [\theta]_N}{[\theta]_D - [\theta]} \quad (1)$$

where $[\theta]$ is the mean residue ellipticity at 222 nm, and $[\theta]_N$ and $[\theta]_D$ are the mean residue ellipticities at 222 nm for the protein in the native and denatured states, respectively.

Preparation of Zinc-Depleted Wild-Type ShhN. Wild-type ShhN (6 mg) was incubated with 200 mg of regenerated CHELEX-100 resin (Bio-Rad, Hercules, CA) in 6 mL of 5 mM Na_2HPO_4, pH 5.5, 0.5 M NaCl, and 0.5 mM DTT for 2 h at room temperature. The resin was removed, and *o*-phenanthroline was added to a concentration of 10 mM. After a further 2 h incubation at room temperature, the protein was dialyzed in Spectra/Por7 metal-free dialysis tubing (Spectrum, Laguna Hills, CA) against 2 × 100 mL of 5 mM Na_2HPO_4, pH 5.5, 0.5 M NaCl, and 0.5 mM DTT with the buffer in the outside chamber containing 1 g of CHELEX-100 resin. Atomic absorption spectroscopy of several preparations indicated a residual zinc content of 0.22−0.37 mol of zinc/mol of protein.

Fluorescence Spectroscopy. GuHCl denaturation studies were performed by incubating ShhN protein (1 μM) overnight at room temperature in 100 mM Hepes, pH 7.5, 150 mM NaCl, and 0.5 mM DTT containing 0.1−3.5 M GuHCl. Similar denaturation measurements were also carried out in the presence of a 10-fold molar excess of EDTA or $ZnSO_4$. Denaturation was monitored by following changes in the intrinsic tryptophan fluorescence of ShhN at excitation and emission wavelengths of 290 and 334 nm, respectively, using an Aminco-Bowman (Rochester, NY) series 2 luminescence spectrometer with the sample holder maintained at 25 °C. Fluorescence intensity was plotted as a function of the GuHCl concentration, and the data were fitted to eq 2, which relates fluorescence intensity to the extent of denaturation based on a two-state model (F = fluorescence intensity, F_N = fluorescence intensity of the native protein, F_D = fluorescence intensity of the denatured protein, [GuHCl] = con-

centration of GuHCl, and *m* and *b* are floating variables):

$$F = \frac{F_N + F_D e^{-((m[\mathrm{GuHCl}]+b/RT))}}{1 + e^{-((m[\mathrm{GuHCl}]+b/RT))}} \quad (2)$$

The free energy of unfolding (ΔG_D), determined from the ratio of native to denatured protein at each GuHCl concentration, was plotted against the GuHCl concentration as described by Pace (*36*). Extrapolation of this plot to zero GuHCl was used to obtain estimates of the free energy of denaturation in the absence of denaturant ($\Delta G_D^{H_2O}$).

The zinc-binding affinity of the zinc-depleted wild-type protein and of the H140A and D147A mutants was determined by titrating solutions of these proteins with $ZnSO_4$ using a fluorescent metal-ion indicator, Magnesium Green, to determine the equilibrium concentration of free zinc present at each concentration of added zinc. Buffers and other solutions were prepared using metal-free water and were stored over CHELEX-100 resin to minimize contamination by adventitious metal ions. To establish the sensitivity of the dye under the relevant conditions, Magnesium Green alone (10 nM) was titrated with a solution of $ZnSO_4$ (in 100 mM Hepes, pH 7.5, and 150 mM NaCl, at 25 °C), and fluorescence was monitored at excitation and emission wavelengths of 506 and 531 nm, respectively. The measured fluorescence intensity showed the expected quadratic dependence on added zinc. Fitting the data to eq 3, in which F is the observed fluorescence intensity; F_{min} and F_{max} are the minimum and maximum fluorescence intensities observed at zero and at very high concentrations of added zinc, respectively; $[Zn^{2+}]$ is total zinc; and [D] is the total concentration of the indicator dye, gave a K_d value of 37 nM for the binding of zinc to the dye, comparable to the value of approximately 20 nM reported by Kuhn et al. (*37*). This established that under the above conditions the levels of zinc in solution could be accurately determined up to concentrations of 200 nM.

$$F = (F_{max} - F_{min}) \times \left\{ \frac{([Zn^{2+}] + [D] + K_d) - \sqrt{([Zn^{2+}] + [D] + K_d)^2 - 4[Zn^{2+}][D]}}{2[D]} \right\} + F_{min} \quad (3)$$

The binding of zinc to the wild-type and mutant proteins was determined by titrating each protein (100 nM) with $ZnSO_4$ to final concentrations of 0−200 nM in the presence of 10 nM Magnesium Green. A standard curve measured in the absence of protein was included in each experiment. The concentration of free zinc present at each concentration of added zinc was determined by reference to this standard curve. The amount of zinc bound to the protein at each concentration of added zinc was then calculated by subtracting free zinc from total zinc, after correction using eq 3 for the small amount of zinc bound to the dye itself. Control experiments showed that the presence of up to 100 nM fully zinc-occupied wild-type protein did not significantly affect either F_{max} or the K_d with which zinc bound to the dye. The zinc titration data were then plotted as $[Zn^{2+}]_{free}$ versus $[Zn^{2+}]_{total}$, and the K_d value for zinc binding to the protein was obtained by fitting the data to eq 4, in which $[Zn^{2+}]_T$ = total zinc, corrected for the small fraction bound to the dye.

$$[Zn^{2+}]_{free} = [Zn^{2+}]_T - \frac{1}{2}\{([Zn^{2+}]_T + [\mathrm{ShhN}] + K_d) - \sqrt{([Zn^{2+}]_T + [\mathrm{ShhN}] + K_d)^2 - 4[Zn^{2+}]_T[\mathrm{ShhN}]}\} \quad (4)$$

^{1}H NMR Spectroscopy. Most NMR experiments were carried out using a Varian (Palo Alto, CA) 600 MHz Unity Inova system using a triple resonance (^{1}H, ^{13}C, and ^{15}N) probe equipped with triple axis pulse field gradient capability. The wild-type and H140A, D147A, and E176A mutant proteins were formulated in 4.5 mM Na_2HPO_4, pH 5.5, 135 mM NaCl, 1 mM DTT, and 10% D_2O at concentrations of 22.5 (1.15 mM), 17.9 (0.92 mM), 22.5 (1.15 mM), and 18.3 mg/mL (0.94 mM), respectively, and were analyzed in Shigemi (Tokyo, Japan) symmetrical NMR microtubes at 20 ± 0.1 °C. For deuterium exchange experiments, protein samples formulated as above were lyophilized to dryness and then resuspended with 100% D_2O. The water signal was suppressed using a solvent presaturation method by irradiating the water signal for 1 s. A total of 256 scans was acquired, with a digital resolution of 0.26 Hz. No line broadening was used during data processing. Chemical shifts were referenced to 2,2-dimethyl-2-silapentane 5-sulfonate, which gives a water resonance at 4.78 ppm. For experiments designed to investigate the effect of metal chelation on wild-type ShhN, the protein was formulated at 22.5 mg/mL (1.15 mM) in 4.5 mM Na_2HPO_4, pH 5.5, 135 mM NaCl, 1 mM DTT, and 11.5 mM EDTA or 11.5 mM *o*-phenanthroline and 10% D_2O, and analyzed with a Varian 500 MHz Unity system. The experimental conditions were essentially the same as those described for the experiments performed with the 600 MHz instrument.

RESULTS

Purification of the Wild-Type and Mutant Proteins. Analysis of the purified wild-type and H140A, D147A, and E176A mutant proteins by SDS−PAGE under reducing conditions and by gel filtration under nonreducing conditions indicated that they were all monomeric (data not shown). ESI−MS analysis indicated that the proteins were intact and had not undergone posttranslational modification; the measured masses of the wild-type and H140A, D147A, and E176A mutant proteins were 19 560, 19 496, 19 517, and 19 502 Da, respectively, in good agreement with the calculated masses of 19 560.02, 19 493.96, 19 516.01, and 19 501.99 Da, respectively. While we were successful in purifying the wild-type and H140A, D147A, and E176A mutants, the H182A mutant proved difficult to purify due to its instability and its susceptibility to cleavage by enterokinase at sites other than at the engineered DDDDK cleavage site. Unlike the histidine-tagged wild-type and E176A proteins that were cleaved only at the DDDDK site, automated Edman N-terminal sequencing indicated that the H182A mutant was cleaved additionally on the carboxy terminal side of residues K45, K54, and R72. Attempts to minimize the nonspecific cleavages by shortening the time of incubation with enterokinase proved unsuccessful as the three truncated species were produced simultaneously with the desired, intact protein. Since the yield of the H182A mutant was low due to this nonspecific cleavage and because even the intact

Table 1: Zinc Content of the Wild-Type and Mutant Proteins

protein	Zn content (mol of Zn/mol of protein)[a]
wild-type	0.99 ± 0.08 (standard deviation)
H140A	0.03 ± 0.01
D147A	0.05 ± 0.02
E176A	1.03 ± 0.03

[a] The zinc content of the wild-type protein is the mean of nine independently formulated samples, while for the mutant proteins the zinc content is the mean of two independently formulated samples.

histidine-tagged protein was unstable and prone to precipitation, no further study of this mutant was made. We also observed that incubation of the histidine-tagged H140A and D147A mutants with enterokinase resulted in the production of minor amounts of three truncated forms. These fragments comigrated on reducing SDS−PAGE gels with those liberated after enterokinase digestion of the histidine-tagged H182A mutant. For the H140A mutant, automated Edman N-terminal sequencing indicated that they resulted from cleavage at the same sites as with the H182A mutant. The time of incubation of the H140A and D147A mutants with enterokinase was therefore limited to no more than 6 h to minimize the undesired cleavages. However, while digestion of the H140A and D147A mutants resulted in the liberation of small amounts of the truncated proteins, the final purified preparations did not contain the clipped forms since they failed to bind to the final SP-Sepharose column used in the purification. ESI−MS analysis confirmed the absence of the clipped forms in the purified preparations of the H140A and D147A mutants (data not shown).

Zinc Content of the Wild-Type and Mutant Proteins. Table 1 shows the zinc content of the wild-type and H140A, D147A, and E176A mutant proteins. Mutation of either of the direct zinc ligands, H140 or D147, to alanine resulted in an almost complete loss of bound zinc (97% and 95%, respectively). By contrast, the E176A mutant had a zinc content of 1 mol of zinc/mol of protein, a value identical to that of the wild-type protein.

In Vitro Biological Activity of the Wild-Type and Mutant Proteins. To determine the effect of zinc occupancy on biological function, the wild-type and mutant proteins were tested for their ability to induce the expression of alkaline phosphatase in C3H10T1/2 cells, a measure of the differentiation of the cells to an osteoblast lineage (*33*), and also for their ability to induce the expression of *islet-1*, a marker for motor neurons, in chick embryo neural plate explants (*34*, *35*).

Figure 1 shows that the alkaline phosphatase inducing activity of the H140A and D147A mutants was reduced significantly as compared to the wild-type protein. By contrast, the activity of the E176A mutant was not significantly different from that of the wild-type protein; both proteins elicit a maximal response at ~10 μg/mL, with EC_{50} values between 1 and 2 μg/mL and between 2 and 3 μg/mL for the wild-type and E176A mutant proteins, respectively. To determine whether the low activity of the H140A and D147A mutants was due to proteolytic degradation during the course of the 5 day assay, 10 μg/mL each of the wild-type protein and the E176A mutant and 10 and 100 μg/mL each of the H140A and D147A mutants were assayed. At the start and at the end of the assay, samples of the culture

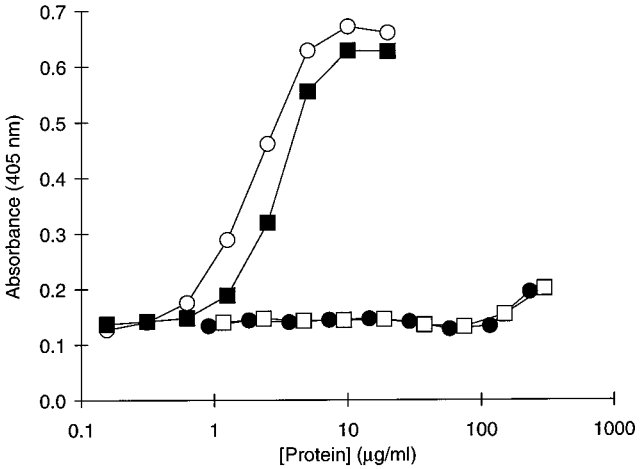

FIGURE 1: Induction of alkaline phosphatase expression in C3H10T1/2 cells. The wild-type and mutant proteins were tested in a cell-based assay measuring the induction of alkaline phosphatase expression, as described in Experimental Procedures. Assays were carried out in duplicate, and the mean values are shown. Data are shown for the wild-type protein (○) and for the H140A (●), D147A (□), and E176A (■) mutants. The mean absorbance value for a control in which no ShhN protein was added was 0.13 ± 0.01.

medium were removed and analyzed by Western blotting. Similar levels of the wild-type protein and the E176A mutant were detected at the start and at the end of the assay. By contrast, when tested at 10 μg/mL, the H140A and D147A mutants were detected only at the start of the assay (data not shown). However, when tested at 100 μg/mL, intact H140A and D147A mutant protein could also be detected at the end of the assay (data not shown). This result suggests that the H140A and D147A mutants are susceptible to proteolytic degradation under the conditions of the assay and that only when tested at a relatively high concentration does a detectable fraction of intact protein survive. We therefore cannot tell whether the low activity of these mutants reflects an intrinsically low activity under the conditions tested or is instead a consequence of their degradation. However, as shown in Figure 1, the observation that they retain some limited activity at concentrations where intact protein remains suggests that they are not totally devoid of activity. Experiments performed in the presence of a cocktail of protease inhibitors showed moderately increased activity for the H140A and D147A mutants, even though in control experiments the inhibitors partially inhibited the response to the wild-type protein (data not shown). When tested in the *islet-1* induction assay, both the H140A and D147A mutants were inactive. Incubation of the explants with the wild-type protein resulted in a mean value of 131 islet-1-positive nuclei per explant, while the H140A and D147A mutants yielded mean values of only 17 and 11 islet-1-positive nuclei per explant, respectively. These values were similar to that obtained with the buffer control, which yielded a mean value of 23 islet-1-positive nuclei per explant. For the E176A mutant, the mean value of 106 islet-1-positive nuclei per explant was similar to that obtained with the wild-type protein. Western blotting analysis of samples of the culture medium removed from the explants at the start and at the end of the assay indicated that, while intact wild-type and E176A protein could be detected at the end of the assay, no H140A or D147A protein could be detected (data not shown). There-

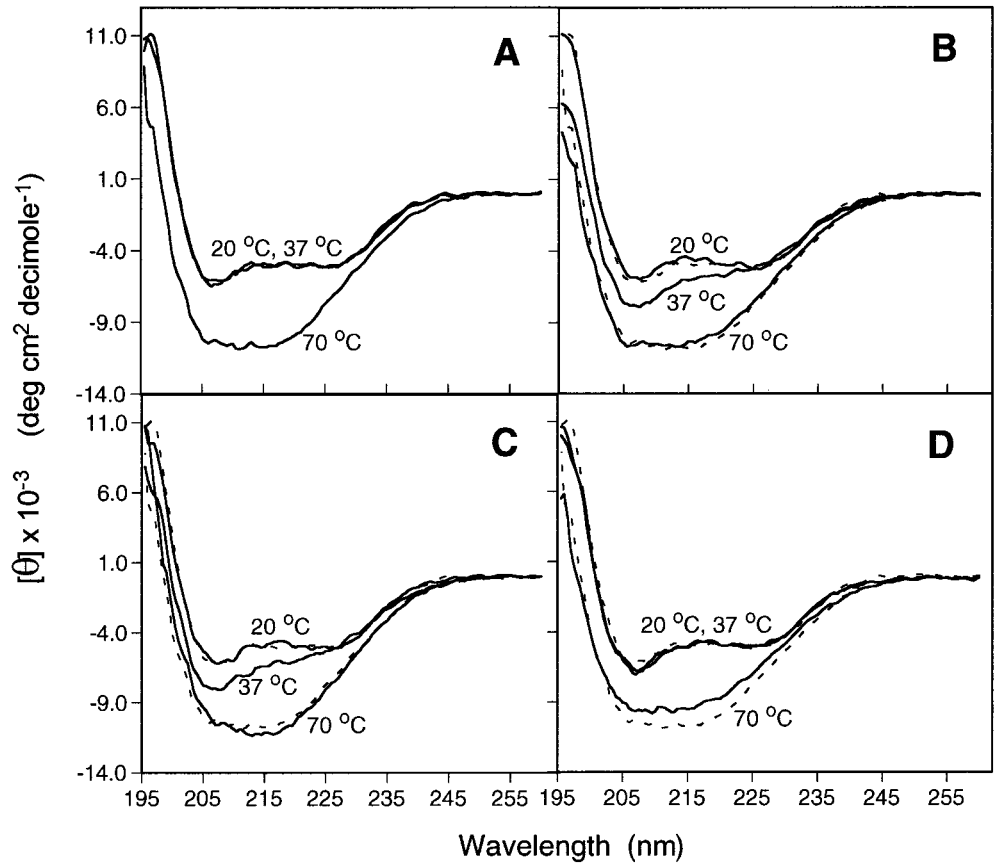

FIGURE 2: CD spectra of the wild-type and mutant proteins measured at 20, 37, and 70 °C. (A) Spectra of the wild-type protein, (B) spectra of the H140A mutant, (C) spectra of the D147A mutant, and (D) spectra of the E176A mutant. For reference, the spectra of the wild-type protein measured at 20 and 70 °C are shown in panels B−D as dashed lines. The procedures used to obtain the spectra are described in Experimental Procedures.

fore, as with the alkaline phosphatase induction assay, it is not possible to say whether the lack of observed activity of the H140A and D147A mutants is due to a low intrinsic activity under the conditions tested or whether it is due to their degradation during the course of the assay.

Thermal Denaturation of the Wild-Type and Mutant Proteins. CD spectroscopy was used to determine how disruption of the zinc-binding site affected the secondary structure of the wild-type and mutant proteins and also their thermal stability. Figure 2 shows the CD spectra of the wild-type and H140A, D147A, and E176A mutant proteins measured at 20, 37, and 70 °C. The CD spectra of the wild-type protein measured at 20 and 37 °C (Figure 2A) indicate that there are no significant structural differences between these two temperatures. By contrast, the spectrum measured at 70 °C (Figure 2A) was significantly different from those measured at 20 and 37 °C and represents that of the fully denatured protein (see below). For the H140A and D147A mutants, the spectra measured at 20 and 70 °C (Figure 2B,C) were very similar to the spectra of the wild-type protein measured at the same temperatures, indicating that at 20 °C there are no detectable structural differences between the wild-type and mutant proteins and that at 70 °C the mutants and the wild-type protein are similarly denatured. However, at 37 °C both the H140A and D147A mutants yielded CD spectra that were intermediate between those measured at 20 and 70 °C (Figure 2B,C), indicating that at this temperature the mutants possess a structure that is somewhat different from that of the native conformation. For the E176A mutant, the spectra measured at 20 and 37 °C (Figure 2D) were very similar to the spectra of the wild-type protein measured at the same temperatures, although at 70 °C the spectra of the denatured wild-type and E176A mutant proteins did not overlie precisely. To understand more fully the effect of the loss of zinc binding on thermal stability, thermal denaturation curves for the wild-type and mutant proteins were obtained over a temperature range of 15−70 °C. Thermal denaturation of the wild-type protein (Figure 3A) followed a single transition starting at ∼52 °C with a T_m value (the temperature at the midpoint of the transition) of ∼59 °C. Similarly, thermal denaturation of the E176A mutant displayed a single transition starting at ∼54 °C with a T_m value of ∼61 °C (Figure 3A). By contrast, thermal denaturation of the H140A mutant (Figure 3A) followed two transitions with T_m values of ∼37 and ∼52 °C, with the first transition starting at ∼34 °C. Likewise, thermal denaturation of the D147A mutant (Figure 3A) followed two transitions with T_m values of ∼38 and ∼54 °C, with the first transition starting at ∼35 °C. Therefore, both the H140A and D147A mutants undergo temperature-dependent structural changes at temperatures 17−18 °C below that at which the wild-type protein first undergoes any detectable structural change. Interestingly, in the presence of a 10-fold molar excess of EDTA, the thermal denaturation of the wild-type protein also displayed two distinct transitions with T_m values of ∼40 and ∼48 °C, with the first transition starting at ∼36 °C. These values are similar to those obtained for the zinc-depleted mutants. To determine whether the addition of zinc would

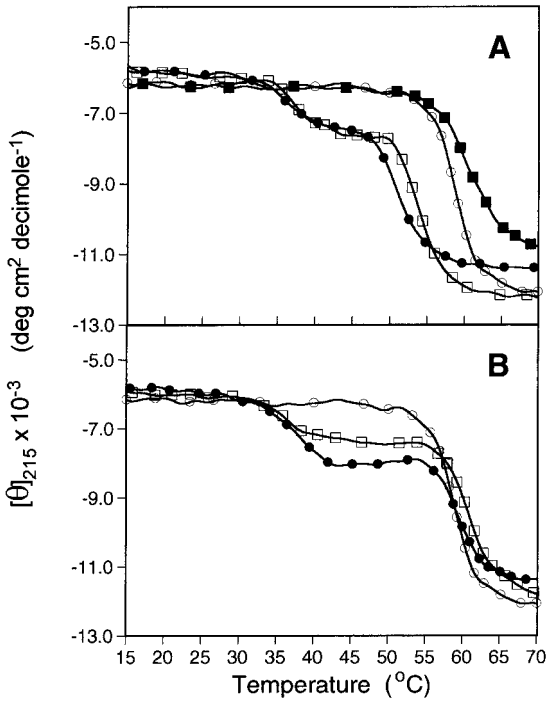

FIGURE 3: Thermal denaturation of the wild-type and mutant proteins as monitored by CD. (A) Melting curves of the wild-type protein (○) and of the H140A (●), D147A (□), and E176A (■) mutants measured in the absence of added $ZnCl_2$. (B) Melting curves of the wild-type protein measured in the absence of added $ZnCl_2$ and of the H140A (●) and D147A (□) mutants measured in the presence of a 16-fold molar excess of $ZnCl_2$. The procedures used to obtain the melting curves are described in Experimental Procedures.

stabilize the H140A and D147A mutants, melting curves were obtained in the presence of a 16-fold molar excess of $ZnCl_2$. Figure 3B shows that the addition of zinc to the H140A and D147A mutants has no significant effect on the first transition; the T_m values measured in the presence of added zinc (~38 and ~36 °C, respectively) were similar to those measured without added zinc (~37 and ~38 °C, respectively). By contrast, zinc increased the T_m value for the second transition by ~7 °C, yielding values of ~59 and ~61 °C for the H140A and D147A mutants, respectively (Figure 3B). These values are essentially identical to the T_m value of the single thermal transition measured for the fully zinc occupied wild-type protein. The ability of added zinc to partially restore thermal stability to the H140A and D147A mutants suggests that the mutants retain the ability to bind zinc, even though in both of these mutants the zinc-binding site that remains is somewhat impaired.

GuHCl-Induced Denaturation of the Wild-Type and Mutant Proteins. GuHCl denaturation studies, using CD and fluorescence spectroscopy, were used to further define the role of zinc in stabilizing the structure of human ShhN. These experiments were performed at 20 (CD) or 25 °C (fluorescence spectroscopy), enabling us to determine the effects of the denaturant independent of the thermal effects described above. While CD analysis indicated that there were no detectable structural differences between the wild-type and mutant proteins at 20 °C, denaturation studies in the presence of GuHCl revealed the extent to which occupancy of the zinc site stabilized the protein structure. Removal of the zinc by the addition of a 10-fold molar excess of EDTA lowered the GuHCl concentration required to give 50% denaturation

Table 2: GuHCl-Induced Denaturation of the Wild-Type and Mutant Proteins in the Absence and Presence of EDTA or $ZnCl_2$ as Monitored by CD[a]

protein	$[GuHCl]_{1/2D}$ (M)
wild-type	1.58
wild-type + EDTA[b]	1.03
H140A	1.04
H140A + $ZnCl_2$[c]	1.56
D147A	1.09
D147A + $ZnCl_2$[c]	1.33
E176A	1.69

[a] The $[GuHCl]_{1/2D}$ values reported in this table were determined from CD measurements as described in Experimental Procedures. [b] The $[GuHCl]_{1/2D}$ was determined in the presence of a 10-fold molar excess of EDTA. [c] The $[GuHCl]_{1/2D}$ was determined in the presence of a 16-fold molar excess of $ZnCl_2$.

($[GuHCl]_{1/2D}$) from ~1.6 to ~1.0 M (Table 2). For the H140A and D147A mutants, the $[GuHCl]_{1/2D}$ values were very similar to that of the EDTA-treated wild-type protein (Table 2), indicating that the loss of zinc from ShhN by either chelation or mutation results in a similar loss of stability in the presence of the denaturant. Addition of a 16-fold molar excess of $ZnCl_2$ to the H140A and D147A mutants largely reversed the destabilization induced by the mutations, as indicated by increases in the $[GuHCl]_{1/2D}$ values (Table 2). For the E176A mutant, the $[GuHCl]_{1/2D}$ value was similar to that of the wild-type protein, indicating that the side chain of E176 does not contribute significantly to structural stability either directly or through its indirect interaction with the zinc ion.

The effect of the mutations on the tertiary structure of the proteins was assessed using fluorescence spectroscopy. In the absence of GuHCl, the fluorescence emission spectra of the mutant proteins were indistinguishable from that of the wild-type protein (data not shown), indicating that the mutations did not cause a detectable change to the microenvironments of the three tryptophan residues present in the protein. However, Figure 4A shows that, in the presence of GuHCl, the H140A and D147A mutants were significantly less stable than the wild-type or E176A mutant proteins. As was observed using CD, the $[GuHCl]_{1/2D}$ values of the H140A (0.47 M) and D147A (0.58 M) mutants were significantly lower than the values of the wild-type protein (1.50 M) and E176A mutant (1.52 M). Although the $[GuHCl]_{1/2D}$ values for the wild-type and E176A mutant proteins measured by CD and fluorescence spectroscopy were similar, the values for the H140A and D147A mutants measured by fluorescence spectroscopy were approximately 0.5 M lower than when measured by CD. These differences might result from the different temperatures used (20 °C for CD versus 25 °C for fluorescence spectroscopy) or may be a consequence of the fact that the two techniques used monitor different aspects of protein structure. Importantly, the overall trend for the destabilization of the mutant proteins is the same irrespective of the technique used. Figure 4A inset shows that when the free energy of unfolding (ΔG_D) is plotted versus the GuHCl concentration and the data extrapolated to zero GuHCl (*36*), the loss of zinc in the H140A and D147A mutants destabilizes the folded protein structure by ~3.5 kcal/mol relative to the wild-type protein. Figure 4B shows that, in the presence of a 10-fold molar excess of EDTA, the denaturation curves of the wild-type

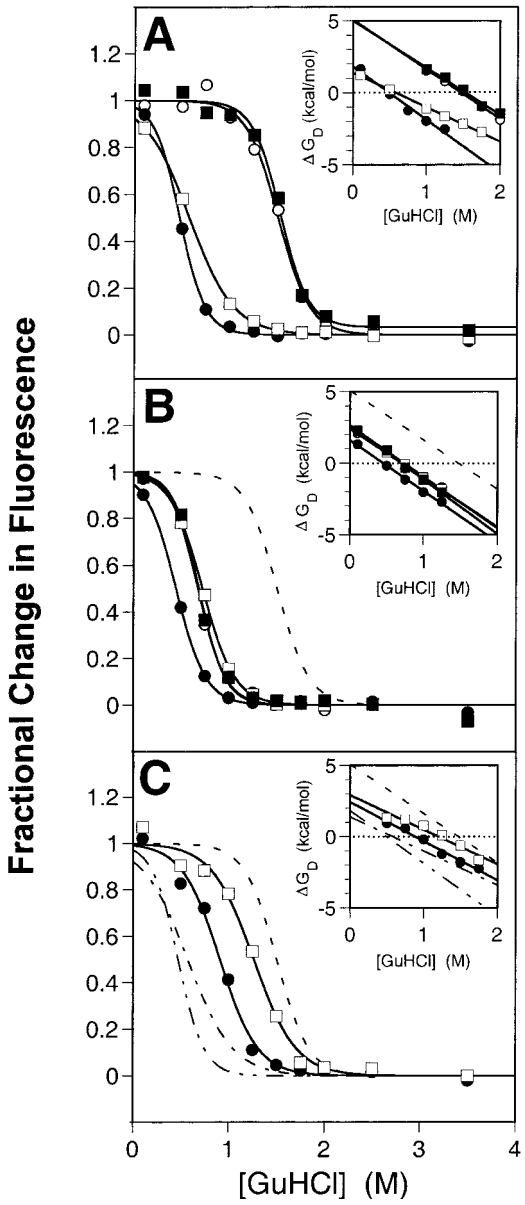

FIGURE 4: GuHCl-induced denaturation of the wild-type and mutant proteins as monitored by fluorescence spectroscopy. The figure shows the denaturation of the wild-type protein (○) and of the H140A (●), D147A (□), and E176A (■) mutants. Data were fitted using eq 2, which relates the change in fluorescence to the extent of protein unfolding, as described in Experimental Procedures. (A) Denaturation curves obtained in the absence of both EDTA and $ZnSO_4$. (B) Denaturation curves obtained in the presence of a 10-fold molar excess of EDTA. For reference, the curve for the wild-type protein obtained in the absence of both EDTA and $ZnSO_4$ is shown as a dashed line. (C) Denaturation curves obtained in the presence of a 10-fold molar excess of $ZnSO_4$. For reference, the curve for the wild-type protein obtained in the absence of both EDTA and $ZnSO_4$ is shown as a dashed line, the curve for the H140A mutant obtained in the absence of both EDTA and $ZnSO_4$ is shown as a dash−dot−dot−dash line, while the curve for the D147A mutant obtained in the absence of both EDTA and $ZnSO_4$ is shown as a dash−dot−dash line. In each panel, the inset plot shows the free energy of unfolding (ΔG_D), calculated for each concentration of GuHCl, plotted as a function of the GuHCl concentration as described in Experimental Procedures. For reference, the dashed line in the inset plots of panels B and C show the free energy of unfolding for the wild-type protein obtained in the absence of both EDTA and $ZnSO_4$, while the dash−dot−dot−dash and dash−dot−dash lines in the inset plot of panel C show the free energy of unfolding for the H140A and D147A mutants, respectively, obtained in the absence of both EDTA and $ZnSO_4$.

and E176A mutant proteins are shifted to lower concentrations of GuHCl, becoming indistinguishable from the denaturation curve of the D147A mutant measured under the same conditions. Figure 4B inset shows that treatment of either the wild-type or E176A mutant protein with EDTA destabilizes the protein structures by ∼3 kcal/mol. This result suggests that the destabilization that results from mutation of H140 or D147 is, in each case, primarily a direct consequence of the loss of zinc rather than arising from any other structural effects. However, the EDTA-treated H140A mutant is destabilized by an additional 0.4−0.8 kcal/mol as compared to the EDTA-treated wild-type, EDTA-treated D147A, or EDTA-treated E176A mutant proteins (Figure 4B), suggesting that mutation of H140 results in some small additional destabilization that is distinct from its effect on zinc binding. Figure 4C shows that adding a 10-fold molar excess of $ZnSO_4$ to the H140A and D147A mutants causes an increase in the $[GuHCl]_{1/2D}$ values corresponding to a partial recovery of the proteins' stability. A similar zinc-induced restoration of stability was observed in the thermal and GuHCl denaturation studies monitored by CD. In none of the GuHCl denaturation studies was any evidence observed for an unfolding intermediate of the kind implied by the biphasic thermal denaturation curves seen for the H140A and D147A mutants (see Figure 3). The conformational state(s) represented by this intermediate therefore do not appear to accumulate at 20 or 25 °C at any of the GuHCl concentrations tested.

Zinc Binding Affinity of the Wild-Type and Mutant Proteins. Since the thermal and GuHCl denaturation studies described above suggested that the H140A and D147A mutants retained some ability to bind zinc, we proceeded to make direct measurements of the zinc-binding affinity of the wild-type and mutant proteins. A fluorescent dye-based zinc-binding assay was developed in which the change in fluorescence of Magnesium Green upon binding zinc was used to monitor the concentration of free zinc present in protein solutions to which various concentrations of zinc had been added. The variation in the free zinc concentration, as zinc was titrated into the protein solutions, was used to determine the extent of zinc binding to the protein. Figure 5 shows that incubation of the H140A and D147A mutants with various concentrations of zinc resulted in plots of $[Zn^{2+}]_{free}$ versus $[Zn^{2+}]_{total}$ that deviated from the linear relationship observed in the absence of protein or in the presence of fully zinc-occupied wild-type ShhN. This deviation results from a fraction of the added zinc binding to the mutant proteins and therefore being unavailable to interact with the indicator dye. Binding of zinc to the H140A and D147A mutants was saturable, as indicated by the fact that at a high concentration of added zinc the data for the mutant proteins becomes linear and parallel to the control curves. Extrapolation of the linear portion of these data to the *x*-axis indicates a stoichiometry of binding of 1 zinc per protein molecule (the *x*-axis intercepts were 96 and 102 nM for the H140A and D147A mutants, respectively, when measured at 100 nM protein). This result was confirmed by performing similar titrations using several different concentrations of the mutant proteins (data not shown). The curve fits shown in Figure 5 indicated that the H140A and D147A mutants bind zinc with K_d values of 1.6 and 15 nM, respectively. Figure 5 inset shows data from a similar experiment in which zinc

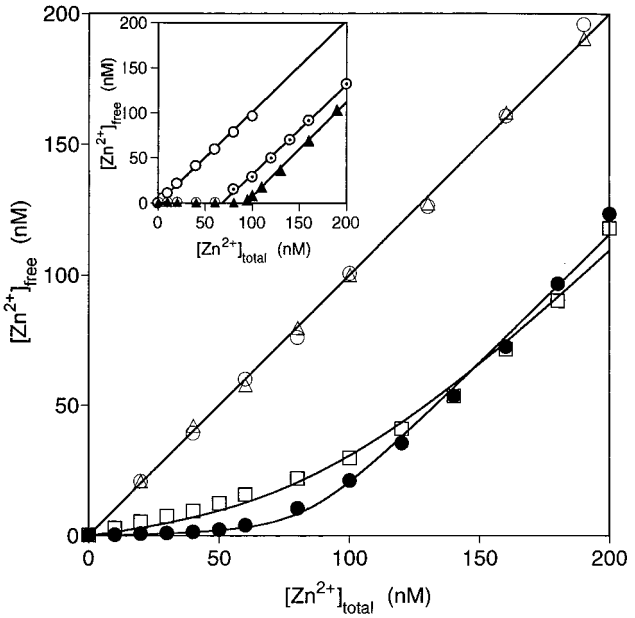

FIGURE 5: Zinc binding affinity of the wild-type and mutant proteins. Titration of $ZnSO_4$ into buffer containing 10 nM Magnesium Green alone (△) or together with 100 nM wild-type protein (○), H140A (●), or D147A (□) mutant protein was performed as described in Experimental Procedures. Data for the mutants were fitted to eq 4, which relates the concentration of free zinc to the concentration of total added zinc and the K_d with which zinc binds to a single site on the protein. The inset plot shows the titration of $ZnSO_4$ into 100 nM wild-type protein (○), 100 nM zinc-depleted wild-type protein (⊙), or 100 nM EDTA (▲).

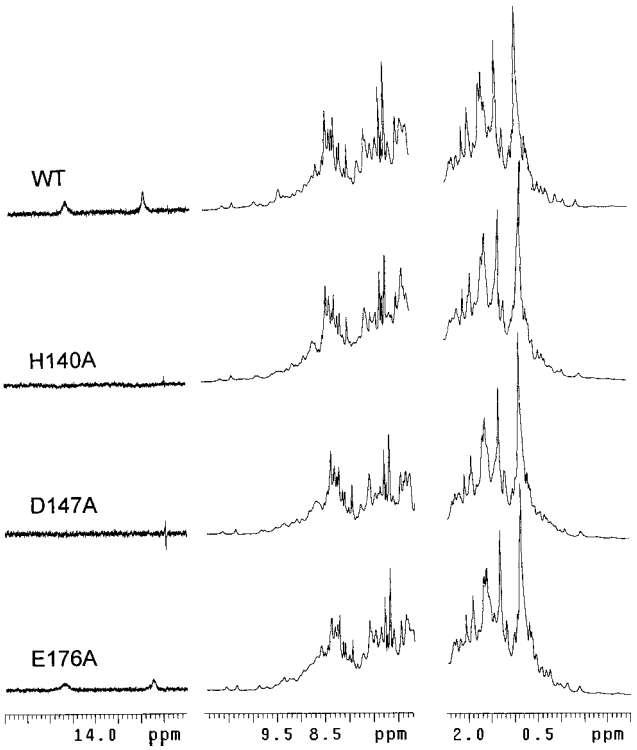

FIGURE 6: ^{1}H NMR spectra of the wild-type protein and of the H140A, D147A, and E176A mutants. The spectral regions spanning −1.5 to 2.5 ppm and 6.7−11 ppm are shown on the same scale, while the regions of the spectra showing the downfield peaks at 13.02 and 14.78 ppm are shown on an expanded scale. The procedures used to obtain the spectra are described in Experimental Procedures.

was titrated against 100 nM zinc-depleted wild-type ShhN or against 100 nM EDTA as a positive control. The data confirmed that about 30% of the zinc-depleted protein was occupied by the metal ion, as was determined independently by atomic absorption spectroscopy. The curve fit established that the zinc-depleted wild-type protein binds zinc with a K_d of ≤100 pM. Taken together, the results in Figure 5 confirmed that the H140A and D147A mutants bind zinc at a single site of relatively high affinity, but that in each case the mutation has caused a substantial weakening of zinc binding relative to the wild-type protein. While we did not determine the affinity with which the E176A mutant bound zinc, the observation that it retains full zinc occupancy during its purification and that, when occupied, the zinc site confers similar stability against thermal and GuHCl-induced denaturation that is seen for wild-type ShhN suggests that it binds zinc with a comparable high affinity to that of the wild-type protein.

^{1}H NMR Spectroscopy of the Wild-Type and Mutant Proteins. ^{1}H NMR analysis of the wild-type and mutant proteins was carried out in order to determine the extent to which the loss of zinc might affect the local tertiary structure of the proteins. As can be seen from Figure 6, the spectra of the wild-type and mutant proteins are very similar, confirming that at 20 °C the loss of zinc in the H140A and D147A mutants does not result in a gross change to the tertiary structure. Moreover, the data obtained for all the proteins showed that good signal dispersion was maintained and therefore that the proteins were folded. While overall the spectra were very similar, small but significant differences were observed between the wild-type and mutant proteins. Most notably, two broad peaks at 13.02 and 14.78 ppm were observed in the spectra of the wild-type and E176A mutant proteins but were absent in the spectra of the H140A and D147A mutants (Figure 6). Since the imide protons of histidine side chains are highly sensitive to their environment and are known to have chemical shifts that vary over a wide range (*38*) and since the side chains of H140 and H182 are involved in zinc binding (*21*), it is possible that the resonances at 13.02 and 14.78 ppm belong to these histidines. To determine whether the loss of the signals at 13.02 and 14.78 ppm reflected the loss of the side chains or was an indirect consequence of the loss of zinc-site structure, additional ^{1}H NMR experiments were carried out in which the wild-type protein was incubated with either EDTA or *o*-phenanthroline. In the presence of either metal chelator, the two downfield peaks were absent (data not shown). NMR data also confirmed that the side chains of these histidines are exposed to bulk solvent, as expected for H140 and H182, since the two downfield peaks disappeared from the spectrum of the wild-type protein after the solvent was replaced with 100% D_2O (data not shown). The two proton peaks at 13.02 and 14.78 ppm are therefore tentatively assigned to the imide protons of the two histidine residues (H140 and H182) involved in zinc binding.

DISCUSSION

Zinc Is Required for the Structural Stability of Human ShhN. Analysis of the crystal structure of murine ShhN shows that the bound zinc is coordinated by two histidines and an aspartate residue (*21*), the same arrangement as that found in *N*-acyl-D-Ala-D-Ala carboxypeptidase (*22*−*24*) and in

D-Ala-D-Ala dipeptidase (*25*, *26*), and similar to that found in thermolysin (*27*, *28*) and in carboxypeptidase A (*29*−*31*). The striking similarity between the coordination of zinc in murine ShhN and in known zinc hydrolases prompted us to investigate the role of zinc in human ShhN. Wild-type human ShhN and mutants carrying H140A, D147A, or E176A substitutions were purified and were characterized with respect to their zinc content, zinc-binding affinity, biological activity, and structural stability.

Determination of the zinc content of the H140A and D147A mutants indicated that H140 and D147 are important for maintaining full zinc occupancy since the mutants retained only 0.03 and 0.05 mol of zinc/mol of protein, respectively, after extensive dialysis (Table 1). Similarly, H116 and D123 in D-Ala-D-Ala dipeptidase, residues which are homologous to H140 and D147 in human ShhN, respectively, have been shown to be critical for full zinc occupancy since the H116A and D123A mutants retained only 0.079 and ≤0.0004 mol of zinc/mol of protein, respectively (*25*). Although we could not purify the H182A mutant of human ShhN and we were therefore unable to determine its zinc content, the fact that it was unstable, coupled with the observation that mutation of H184 to alanine in D-Ala-D-Ala-dipeptidase (the homologous residue to H182 in human ShhN) resulted in an enzyme with only 0.0092 mol of zinc/mol of protein (*25*), suggests that it too would be zinc-deficient. While mutation of the residues directly involved in coordinating the zinc resulted in significant losses of the metal ion, mutation of E176 to alanine in human ShhN had no effect on zinc occupancy (Table 1). This indicates that the indirect interaction between the side chain of E176 and the zinc ion, which is mediated via a zinc-bound water molecule, is not essential for high affinity binding of the metal ion. Similarly, mutation of E181 to alanine in D-Ala-D-Ala dipeptidase (the homologous residue to E176 in human ShhN) indicated that the side chain of E181 had no significant effect on zinc occupancy (*25*).

The biophysical analyses used in this study to investigate the structure of the wild-type and mutant proteins show that, in the presence of GuHCl, loss of zinc binding either by treatment with EDTA or by mutation of the direct zinc ligands H140 and D147 causes a substantial reduction in the proteins' stability against denaturation. As determined by CD and fluorescence spectroscopy, the $[GuHCl]_{1/2D}$ values are lower by 0.5−1 M for the H140A and D147A mutants as compared to the wild-type protein, while for the E176A mutant, which has full zinc occupancy, there was no reduction in stability. Thermal denaturation studies showed that at temperatures below ∼35 °C the native structures of the H140A, D147A, and E176A mutants are overall very similar to that of the wild-type protein. At 20 or 25 °C, the CD, fluorescence, and ^{1}H NMR spectra of the mutants are essentially identical to that of the wild-type protein. These results indicate that, at these temperatures, the absence of zinc does not, in itself, result in gross changes in secondary or tertiary structure. However, at higher temperatures the effect of zinc depletion becomes apparent. For the wild-type and E176A mutant proteins, the bound zinc stabilizes the protein structure such that they do not begin to unfold until 52−54 °C, after which they denature by means of a single thermal transition (Figure 3A). By contrast, the H140A and D147A mutants begin to undergo conformational changes at much lower temperatures, whereupon unfolding from the native to the fully denatured state displays two distinct thermal transitions. The second thermal transition likely represents the global unfolding of the protein since it comprises the majority of the observed structural change and, in the presence of added zinc, occurs at a temperature similar to that for the single thermal transition observed for the wild-type and E176A mutant proteins. However, it is not clear what conformational state(s) the H140A and D147A mutants exist in after the first thermal transition. While this transition (T_m 37−38 °C) is clearly related to perturbation of the zinc site, it is noteworthy that occupancy of the impaired zinc site in the H140A and D147A mutants does not affect the T_m value of the first transition while it clearly affects the second. Biological assay of the wild-type and mutant proteins at 37 °C indicates that the H140A and D147A mutants are significantly less active than the wild-type protein, while the E176A mutant has similar activity to the wild-type protein. Although we cannot determine the exact cause of the reduced activity of the H140A and D147A mutants, it is likely to be due either to the unfolding intermediates detected at this temperature having an intrinsically lower activity than their native states or to these conformations being susceptible to proteolysis under the conditions of the assay.

The above results establish the following picture of the structural role of the zinc site in human ShhN. Zinc stabilizes the native structure by approximately 3−3.5 kcal/mol. Loss of this stabilization, either by removal of the zinc from the wild-type protein with EDTA or by mutagenesis of the zinc-binding site, does not result in significant changes to the average secondary or tertiary structure at 20−25 °C as detected by CD, fluorescence, and ^{1}H NMR spectroscopies. However, at temperatures between ∼35 and ∼50 °C, loss of zinc binding causes the adoption of a new structure that is distinct from that of the native protein although it retains considerable secondary structure. This finding may account for the increased susceptibility to proteolysis seen with the H140A and D147A mutants. The direct zinc ligands H140 and D147 contribute substantially to the zinc-binding affinity of the protein ($\Delta\Delta G$ >3 and >4.4 kcal/mol, respectively, at 25 °C), and their mutation weakens zinc binding to the extent that the H140A and D147A mutants purified as *Apo* proteins. However, replacement of either one of these residues by alanine results in a zinc site that, though impaired, still retained the ability to bind zinc with low nanomolar affinity and that, when occupied by zinc, partially restored the protein's stability against thermal or GuHCl-induced denaturation. These results are consistent with those of Kiefer and Fierke (*39*), who showed that mutating the histidine residues that are direct zinc ligands in carbonic anhydrase II substantially reduced zinc-binding affinity but that the resulting impaired zinc sites were still able to bind zinc with submicromolar affinity. By contrast, the indirect interaction of E176 with the zinc ion, which in the crystal structure of murine ShhN is mediated by a bridging water molecule, does not contribute significantly to stabilizing the interaction between the protein and the zinc ion, and therefore mutation of E176 to alanine has no measurable effect on the stability of the protein against denaturation.

Zinc Hydrolase Activity Is Not Required for the In Vitro Biological Function of Human ShhN. The structural similarity between the zinc site found in murine ShhN and that found

in known zinc hydrolases raised the possibility that murine ShhN might possess metalloprotease activity (*21*). However, murine ShhN was unable to catalyze the hydrolysis of a C-terminal peptide corresponding to residues E189 through to G198 (*21*), a candidate substrate suggested by crystal packing interactions. We attempted to broaden the search for a hydrolase activity for ShhN by testing various proteins and peptides as substrates. Assays based on the hydrolysis of biotinylated gelatin, azoalbumin, or agarose-embedded casein could detect thermolysin activity at concentrations as low as 3 nM. By contrast, there was no detectable hydrolysis of these proteins by 1 μM wild-type human ShhN under similar conditions (Moore and Whitty, unpublished observations). To determine whether human ShhN might be a dipeptidase similar to D-Ala-D-Ala dipeptidase (*25*), the protein was assayed using various commercially available D- or L-alanine containing di- and tripeptides as substrates. As with the protein substrates described above, no hydrolytic activity was detected with any of the peptides tested (Day and Whitty, unpublished observations).

As an alternative approach to determining whether human ShhN might be a zinc hydrolase, we mutated E176 to alanine. E176 in human ShhN is structurally analogous to E143 in thermolysin (*27*), to E270 in carboxypeptidase A (*29*), to E181 in D-Ala-D-Ala dipeptidase (*26*), and to H192 in *N*-acyl-D-Ala-D-Ala carboxypeptidase (*22*, *26*), residues that are believed to function by activating the zinc-bound water molecule for attack on the protein-bound substrate. Since mutation of E181 to alanine in D-Ala-D-Ala dipeptidase resulted in an inactive enzyme (*25*), if human ShhN was dependent upon hydrolase activity for biological function it was considered likely that the E176A mutant would be significantly less active than the wild-type protein. Analysis of the E176A mutant offered the best opportunity to address this issue because mutation of the three direct zinc ligands (H140, D147, and H182) resulted in proteins with reduced stability.

The E176A mutant showed no significant decrease in the ability to induce the expression of alkaline phosphatase in C3H10T1/2 cells as compared to the wild-type protein (Figure 1), confirming results obtained with the unpurified mutant expressed and secreted from COS cells (Garber et al., unpublished observations), or to induce the expression of *islet-1* in chick embryo neural plate explants. These results indicate that hydrolase activity is not required for the function of human ShhN in these in vitro assays, which measure the ability of the protein to induce cell differentiation. There is thus no compelling reason to assume that zinc hydrolase activity is essential for the numerous roles that ShhN plays during embryo development. The structure of the zinc site in human ShhN may therefore simply reflect the evolutionary retention of structural features derived from an ancestral zinc hydrolase for reasons other than a requirement for catalysis. For example, it is possible that the zinc site might function as the binding site for other proteins that interact with ShhN. Human ShhN may therefore represent an example of enzymes or enzyme-like molecules that serve functions other than those requiring catalysis. Other examples of this phenomenon include crystallin proteins of the eye that have been shown to be encoded by the same genes that encode enzymes such as lactate dehydrogenase, aldehyde dehydrogenase, glutathione transferase, and transketolase (*40*, *41*). Tyrosyl-tRNA synthetase, an enzyme that catalyzes the attachment of tyrosine to its corresponding tRNA, has been shown to undergo proteolytic cleavage to yield two fragments, both of which are functional cytokines (*42*). Similarly, aconitase has been shown to be an iron-responsive RNA binding protein that regulates the stability of transferrin and transferrin receptor mRNA in addition to its catalytic role in the citric acid cycle (*43*). However, despite the evidence that indicates that hydrolase activity is not required for the in vitro biological activity of human ShhN, we cannot rule out the possibility that the protein has a catalytic role in its natural in vivo setting and that this activity is important for embryo development. To address this possibility, experiments are underway to replace the wild-type *Shh* gene in mice with a gene encoding the E177A mutant to determine whether loss of the postulated catalytic base has any affect on embryo development, either in a tissue-specific and/or developmental stage-dependent manner (Dr. Gord Fishell, personal communication).

In summary, mutation of H140, D147, and H182 to alanine in human ShhN results in mutants with significantly reduced stability as compared to the wild-type protein. For the H140A and D147A mutants, which could be purified, the loss of stability, susceptibility to proteolytic degradation, and decreased in vitro biological activity correlated with the loss of zinc-binding affinity. By contrast, mutation of E176 to alanine resulted in a mutant protein with wild-type zinc occupancy, structural stability, resistance to proteolytic degradation, and in vitro biological activity. The normal levels of biological activity of the E176A mutant indicates that, despite its resemblance to the enzymes D-Ala-D-Ala-dipeptidase, *N*-acyl-D-Ala-D-Ala-carboxypeptidase, thermolysin, and carboxypeptidase A, zinc hydrolase activity is not required for the in vitro activity of human ShhN. These results therefore suggest that the zinc-binding site in ShhN plays primarily or exclusively a structural role.

ACKNOWLEDGMENTS

We thank Richard Tizard, Janice Nelson, Christopher Tonkin, Michele McAuliffe, and Brittney Coleman for sequencing DNA; Dr. Stephan Miller for arranging for the expression of wild-type ShhN at Rutgers University; Dr. Blake Pepinsky for assisting in the purification of wild-type ShhN; and Dr. David Bumcrot (Ontogeny Inc.) for providing plasmid p6H-SHH. We also thank one of the anonymous reviewers for their comments concerning the thermal stability of the mutant proteins that led to a significantly improved manuscript.

REFERENCES

1. Marigo, V., Roberts, D. J., Scott, M. K. L., Tsukurov, O., Levi, T., Gastier, J. M., Epstein, D. J., Gilbert, D. J., Copeland, N. G., Seidman, C. E., Jenkins, N. A., Seidman, J. G., McMahon, A. P., and Tabin, C. (1995) *Genomics 28*, 44−51.
2. Hammerschmidt, M., Brook, A., and McMahon, A. P. (1997) *Trends Genet. 13*, 14−21.
3. Echelard, Y., Epstein, D. J., St-Jacques, B., Shen, L., Mohler, J., McMahon, J. A., and McMahon, A. P. (1993) *Cell 75*, 1417−1430.
4. Roelink, H., Porter, J. A., Chiang, C., Tanabe, Y., Chang, D. T., Beachy, P. A., and Jessell, T. M. (1995) *Cell 81*, 445−455.

5. Ericson, J., Morton, S., Kawakami, A., Roelink, H., and Jessell, T. L. (1996) *Cell 87*, 661−673.
6. Hynes, M. A., Porter, J. A., Chiang, C., Chang, D., Tessier-Lavigne, M., Beachy, P. A., and Rosenthal, A. (1995) *Neuron 15*, 35−44.
7. Wang, M. Z., Jin, P., Bumcrot, D. A., Marigo, V., McMahon, A. P., Wang, E. A., Woolf, T., and Pang, K. (1995) *Nat. Med. 1*, 1184−1188.
8. Ericson, J., Muhr, J., Placzek, M., Lints, T., Jessell, T. M., and Edlund, T. (1995) *Cell 81*, 747−756.
9. Pepicelli, C. V., Lewis, P. M., and McMahon, A. P. (1998) *Curr. Biol. 8*, 1083−1086.
10. Jensen, A. M., and Wallace, V. A. (1997) *Development 124*, 363−371.
11. Levine, E. M., Roelink, H., Turner, J., and Reh, T. A. (1997) *J. Neurosci. 17*, 6277−6288.
12. Belloni, E., Muenke, M., Roessler, E., Traverso, G., Siegel-Bartelt, J., Frumkin, A., Mitchell, H. F., Donis-Keller, H., Helms, C., Hing, A. V., Heng, H. H. Q., Koop, B., Martindale, D., Rommens, J. M., Tsui, L.-C., and Scherer, S. W. (1996) *Nat. Genet. 14*, 353−356.
13. Roessler, E., Belloni, E., Gaudenz, K., Jay, P., Berta, P., Scherer, S. W., Tsui, L.-C., and Muenke, M. (1996) *Nat. Genet. 14*, 357−360.
14. Roessler, E., Ward, D. E., Gaudenz, K., Belloni, E., Scherer, S. W., Donnai, D., Siegel-Bartelt, J., Tsui, L.-C., and Muenke, M. (1997) *Human Genet. 100*, 172−181.
15. Chiang, C., Litingtung, Y., Lee, E., Young, K., Corden, J. L., Westphal, H., and Beachy, P. A. (1996) *Nature 383*, 407−413.
16. Lee, J. J., Ekker, S. C., von Kessler, D. P., Porter, J. A., Sun, B. I., and Beachy, P. A. (1994) *Science 266*, 1528−1537.
17. Bumcrot, D. A., Takada, R., and McMahon, A. P. (1995) *Mol. Cell. Biol. 15*, 2294−2303.
18. Porter, J. A., Ekker, S. C., Park, W.-J., von Kessler, D. P., Young, K. E., Chen, C.-H., Ma, Y., Woods, A. S., Cotter, R. J., Koonin, E. V., and Beachy, P. A. (1996) *Cell 86*, 21−34.
19. Porter, J. A., Young, K. E., and Beachy, P. A. (1996) *Science 274*, 255−259.
20. Pepinsky, R. B., Zeng, C., Wen, D., Rayhorn, P., Baker, D. P., Williams, K. P., Bixler, S. A., Ambrose, C. M., Garber, E. A., Miatkowski, K., Taylor, F. R., Wang, E. A., and Galdes, A. (1998) *J. Biol. Chem. 273*, 14037−14045.
21. Tanaka Hall, T. M., Porter, J. A., Beachy, P. A., and Leahy, D. J. (1995) *Nature 378*, 212−216.
22. Wery, J. D. (1987) Ph.D. Thesis, University of Leige.
23. Ghuysen, J. M. (1988) *Antibiotic Inhibition of Bacterial Cell Surface Assembly and Function* (Actor, P., Ed.) American Society for Microbiology, Washington, DC.
24. Murzin, A. G. (1996) *Curr. Opin. Struct. Biol. 6*, 386-394.
25. McCafferty, D. G., Lessard, I. A. D., and Walsh, C. T. (1997) *Biochemistry 36*, 10498−10505.
26. Bussiere, D. E., Pratt, S. D., Katz, L., Severin, J. M., Holzman, T., and Park, C. H. (1998) *Mol. Cell 2*, 75−84.
27. Holmes, M. A., and Matthews, B. W. (1982) *J. Mol. Biol. 160*, 623−629.
28. Hangauer, D. G., Monzingo, A. F., and Matthews, B. W. (1984) *Biochemistry 23*, 5730−5741.
29. Rees, D. C., Lewis, M., and Lipscomb, W. N. (1983) *J. Mol. Biol. 168*, 367−387.
30. Christianson, D. W. (1991) *Adv. Protein Chem. 42*, 281−355.
31. Bukrinsky, J. T., Bjerrum, M. J., and Kadziola, A. (1998) *Biochemistry 37*, 16555−16564.
32. Gill, S. C., and von Hippel, P. H. (1989) *Anal. Biochem. 182*, 319−326.
33. Nakamura, T., Aikawa, T., Iwamoto-Enomoto, M., Iwamoto, M., Higuchi, Y., Maurizio, P., Kinto, N., Yamaguchi, A., Noji, S., Kurisu, K., and Matsuya, T. (1997) *Biochem. Biophys. Res. Commun. 237*, 465−469.
34. Yamada, T., Pfaff, S. L., Edlund, T., and Jessell, T. M. (1993) *Cell 73*, 673−686.
35. Tanabe, Y., Roelink, H., and Jessell, T. M. (1995) *Curr. Biol. 5*, 651−658.
36. Pace, C. N. (1986) *Methods Enzymol. 131*, 266−280.
37. Kuhn, M. A., Hoyland, B., Carter, S., Zhang, C., and Haugland, R. P. (1995) *Proc. Int. Soc. Opt. Eng. 2388*, 238−244.
38. Wishart, D. S., Richards, F. M., and Sykes, B. D. (1991) *J. Mol. Biol. 222*, 311−333.
39. Kiefer, L. L., and Fierke, C. A. (1994) *Biochemistry 33*, 15233−15240.
40. Hendriks, W., Mulders, J. W. M., Bibby, M. A., Slingsby, C., Bloemendal, H., and de Jong, W. W. (1988) *Proc. Natl. Acad. Sci. U.S.A. 85*, 7114−7118.
41. Piatigorsky, J. (1998) *Ann. N. Y. Acad. Sci. 842*, 7−15.
42. Wakasugi, K., and Schimmel, P. (1999) *Science 284*, 147−151.
43. Rouault, T., and Klausner, R. (1997) *Curr. Top. Cell. Regul. 35*, 1−19.

BI9910068